

THE OFFICIAL MAGAZINE OF THE OCEANOGRAPHY SOCIETY

Oceanography

CITATION

Lavelle, J.W., A.M. Thurnherr, L.S. Mullineaux, D.J. McGillicuddy Jr., and J.R. Ledwell.
2012. The prediction, verification, and significance of flank jets at mid-ocean ridges.
Oceanography 25(1):277–283, <http://dx.doi.org/10.5670/oceanog.2012.26>.

DOI

<http://dx.doi.org/10.5670/oceanog.2012.26>

COPYRIGHT

This article has been published in *Oceanography*, Volume 25, Number 1, a quarterly journal of The Oceanography Society. Copyright 2012 by The Oceanography Society. All rights reserved.

USAGE

Permission is granted to copy this article for use in teaching and research. Republication, systematic reproduction, or collective redistribution of any portion of this article by photocopy machine, reposting, or other means is permitted only with the approval of The Oceanography Society. Send all correspondence to: info@tos.org or The Oceanography Society, PO Box 1931, Rockville, MD 20849-1931, USA.



The Prediction, Verification, and Significance of Flank Jets at Mid-Ocean Ridges

BY J. WILLIAM LAVELLE, ANDREAS M. THURNHERR, LAUREN S. MULLINEAUX,
DENNIS J. MCGILLICUDDY JR., AND JAMES R. LEDWELL

ABSTRACT. One aspect of ocean flow over mid-ocean ridges that has escaped much attention is the capacity of a ridge to convert oscillatory flows into unidirectional flows. Those unidirectional flows take the form of relatively narrow jets hugging the ridge's flanks. In the Northern Hemisphere, the jets move heat and dissolved and particulate matter poleward on the west and equatorward on the east of north-south trending ridges. Recent measurements and a model of flow at the East Pacific Rise at 9–10°N show that these ridge-parallel flows can extend 10–15 km horizontally away from the ridge axis, reach from the seafloor to several hundreds of meters above ridge crest depth, and have maximum speeds in their cores up to 10 cm s⁻¹. Because of their along-ridge orientation and speed, the jets can significantly affect the transport of hydrothermal vent-associated larvae between vent oases along the ridge crest and, possibly, contribute to the mesoscale stirring of the abyssal ocean. Because jet-formation mechanisms involve oscillatory currents, ocean stratification, and topography, the jets are examples of “stratified topographic flow rectification.” Ridge jets have parallels in rectified flows at seamounts and submarine banks.

BACKGROUND

Motion near the deep ocean floor is often thought to be sluggish, and to change only gradually with distance. Such a view is far from reality, however, in areas of strong topographic relief. The 67,000 km global ribbon of tectonic plate spreading centers, where the process of creating new seafloor has built submarine mountain ridges, is one locale where abyssal ocean currents are surprisingly energetic. A broad spectrum of oscillatory flows are amplified in the vicinity of the ridge (e.g., Thomson et al.,

1990; Allen and Thomson, 1993; Lavelle and Cannon, 2001), temperature and salinity distributions are often perturbed in a way that causes them to dome above a ridge (e.g., Thurnherr et al., 2011), and long-term averaged flows can be dominated by narrow, depth-limited, and relatively strong current streams that flow alongside the ridge. These flank jets are the focus of this article.

Though flank jets are likely present at many submarine ridges, only a few observational studies have been made with spatial resolution fine enough

to detect them. Single current meters placed on opposite sides of the Juan de Fuca Ridge (JdFR) by Cannon et al. (1991) provided the first evidence that mean flows were alongside the ridge and directionally sheared across it. These authors' time-integrated the velocity measurements to approximate particle trajectories and showed with just two trajectories that currents were northward on the west side and southward on the east side of the ridge. To look more closely at ridge adjacent flow, Cannon and Pashinski (1997) deployed 11 moorings on a transect across the JdFR at 45°N, each mooring hosting a single current meter, all at nearly ridge-crest depth. The resulting three-month averaged flow showed not only a directional shear across the ridge in the sense of the earlier measurements, but that the distributions of along-ridge mean velocity distributions were nearly anti-symmetric (poleward to the west) across the ridge, with speed maxima of 3 cm s⁻¹ at a distance of ~ 15 km from the ridge crest. At a distance of ± 20 km off axis, the along-ridge flows had all but disappeared. Spreading-center flank jets were emerging from the observations.

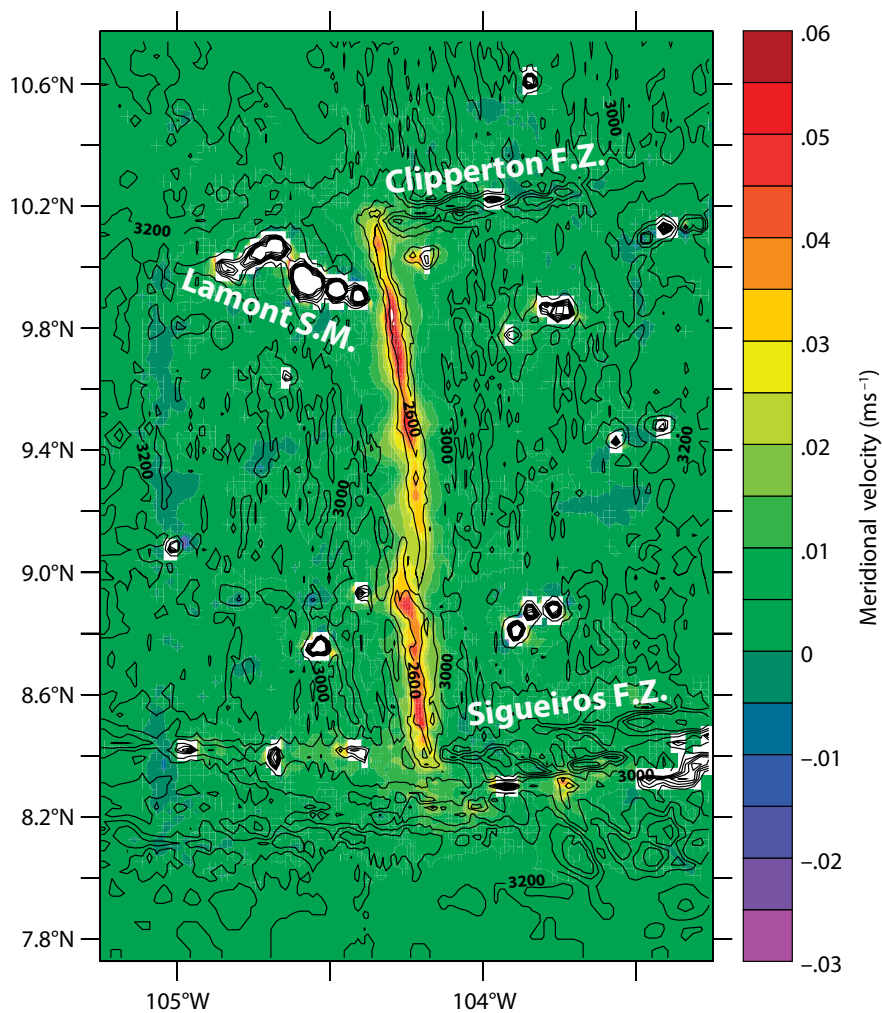


Figure 1. Bathymetry in the region of the East Pacific Rise 9–10°N depicted in contours (black). The ridge crest has a depth of approximately 2,550 m. The Lamont Seamounts and the Clipperton Fracture Zone are found near the northern end of this ~ 200 km long mid-ocean ridge spreading center segment; the Siqueiros Fracture Zone is east of the southern tip. Instantaneous meridional velocities (positive northward) at a depth of 2,500 m, based on a three-dimensional model simulation, are color contoured. The poleward meridional flank jet depicted with hotter colors is nearly discontinuous at ~ 9°N where the ridge topography provides evidence of an overlapping spreading center.

DETECTION AT THE EAST PACIFIC RISE (EPR)

When the chance to measure ocean currents along the East Pacific Rise (EPR) at 9–10°N (Figure 1) came along in 2006, it was not clear whether similar along-ridge mean currents might be found there. Differences between the EPR and JdFR sites are considerable. A major difference is site latitude, which scales the very important Coriolis force, the product of velocity and a latitude-dependent factor due to Earth's rotation. For the same current velocity, the Coriolis force is more than four times larger ($\sin 45^\circ/\sin 9.5^\circ$) at the JdFR at 45°N than at the EPR at 9.5°N. Site latitude also determines which incident waves are amplified in the vicinity of the ridge (waves whose periods exceed $12 \text{ hr}/\sin[\text{latitude}]$; i.e., subinertial waves) and which are not (see, e.g., Lavelle and Mohn, 2010). Of the two sites, only at the JdFR are diurnal waves subinertial. Would that difference prove important to jet formation? Moreover, ocean currents incident on each of the two ridges have substantially different frequency spectra, with 35% of the energy at the EPR 9–10°N having periods > 200 hr, while at Axial Volcano on the JdFR, for example, that same spectral band accounts for < 3% of the total energy. Regional ocean stratification profiles differ as well. Preliminary two-dimensional model results suggested flank jets would exist at the EPR site, too, but that didn't quell the doubts of some on the science team. Would jets have significant enough size and magnitude to be observed? And, even if found, would the length scales, height, width, and magnitude of the jets be anything like the model's prediction?

J. William Lavelle (j.william.lavelle@noaa.gov) is Physical Oceanographer, National Oceanic and Atmospheric Administration Pacific Marine Environmental Laboratory, Seattle, WA, USA. **Andreas M. Thurnherr** is Lamont Associate Research Professor, Division of Ocean and Climate Physics, Lamont-Doherty Earth Observatory, Palisades, NY, USA. **Lauren S. Mullineaux** is Senior Scientist, Biology Department, Woods Hole Oceanographic Institution, Woods Hole, MA, USA. **Dennis J. McGillicuddy Jr.** is Senior Scientist, Applied Ocean Physics and Engineering Department, Woods Hole Oceanographic Institution, Woods Hole, MA, USA. **James R. Ledwell** is Senior Scientist, Applied Ocean Physics and Engineering Department, Woods Hole Oceanographic Institution, Woods Hole, MA, USA.

BOX 1 | THE HUNT FOR SF₆ AND THE EFFECT OF THE LAMONT SEAMOUNT CHAIN

In 2006–2007, the LADDER (LARval Dispersion along the Deep East Pacific Rise) group undertook three expeditions to the EPR 9–10°N site to study a variety of physical and biological phenomena. Thurnherr et al. (2011) describe repeated conductivity, temperature, depth velocity profiles and data from nine current meter moorings that collected year-long measurements. Jackson et al. (2010) present measurements of the tracer sulfur hexafluoride (SF₆) released 30 days prior above the ridge axis at 9.5°N (see Box 1). Mullineaux et al. (2010) discuss how recovered larvae and newly settled juveniles from plankton and seafloor samples signaled a change in the vent species mix at the 9°50'N site following the lava eruption of 2005. Results from the ship-based current velocity survey, after tidal currents had been accounted for, did indeed show poleward mean flow to the west and equatorward mean flow to the east of the ridge. Velocities were in the range of 2–6 cm s⁻¹. More tellingly, a profiling current meter moored 10 km west of the ridge showed features of the near-ridge, along-isobath flow that had not been observed before (Thurnherr et al., 2011). Currents were intensified not only at ridge-crest depth but also at depths from several hundred meters above the ridge nearly to the seafloor. Moreover, those data, when binned into weekly averages, showed maximal jet speed at the site 10 km off axis that varied from < 1 cm s⁻¹ to as much as 10 cm s⁻¹. The hydrographic transect showed isotherms and isopycnals (lines of equal density) that were elevated (domed) over the ridge crest, and that crept up the flank on one side and plunged downward into the flank on the opposite side of the ridge

Sulfur hexafluoride (SF₆) gas has become an important tool for tracing ocean transport due to its low ambient ocean concentrations, high detection sensitivity, and high solubility (Watson and Ledwell, 2000). During the first LADDER expedition, 3 kg of SF₆ were released just above the EPR at 9.5°N with the idea that its dispersion would emulate the dispersion of non- and weakly swimming hydrothermal vent-originating larvae (Jackson et al., 2010). The hunt for the injected SF₆ was taken up 30 days later, and surprises about its evolving location were immediate. Only a very small fraction of the injection could be found along the ridge crest to the north, and none was found to the south. A search along the Clipperton Fracture Zone (Figure 1), located east of the ridge's northern tip, also came up blank. It was only when researchers began taking water samples well to the west of the ridge in and around the western Lamont Seamounts that the bulk of the initial tracer SF₆ release could be accounted for (Figure B-1). That SF₆ data quickly altered our perspective on the timescales for transport along the ridge and about the importance to dispersion of off-ridge, nearby topography like the seamounts. Previous studies had assumed that any larvae transported 25 km or more away from the ridge would be lost to the abyssal ocean (Marsh et al., 2001), but the SF₆ tracer showed that some could return to habitable vents on the ridge. The numerical model of circulation and transport subsequently helped us understand why the SF₆ cloud evolved as it did (Lavelle et al., 2010). Model results imply that the tracer moved rapidly north in the westward ridge jet until it reached the gap between the seamounts and the ridge. Just at that time, a short-term reversal in regional current direction blocked SF₆ movement through the passage, putting the tracer on a path to the west, just south of the seamounts. Later, a longer-term directional reversal of regional flow sent the SF₆ back toward the ridge. The conclusion of the combined field and model studies is that dispersion pathways at this EPR segment depend on the flank jets, the seamounts, and on directional variability of regional flow. Those connections would be much less well appreciated were it not for SF₆ tracer methodology and results.

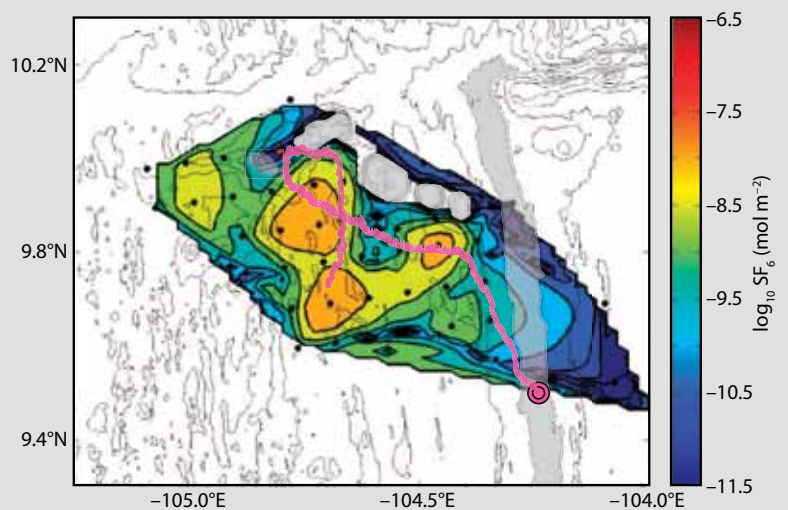


Figure B-1. Vertically integrated SF₆ concentrations ranging from 3.2×10^{-7} to 3.2×10^{-12} mol m⁻² measured at conductivity, temperature, depth (CTD) stations (black dots) 42 to 52 days after the SF₆ was released on the ridge at 9.5°N (purple circle). The superimposed trajectory (purple) is a model estimate of the center of mass of the SF₆ over time. The East Pacific Rise and Lamont Seamounts are highlighted in gray.

(Thurnherr et al., 2011). The SF₆ tracer experiment led to an interpretation (see Box 1) that also confirmed the existence and importance of flank jets along this ridge segment. The flank jet skeptics were converted.

MODEL EXTRAPOLATIONS

Measurements at the EPR led to additional two- and three-dimensional numerical modeling work on ridge-influenced and regional flow. Models were forced in a way to make model currents resemble measured currents at the ridge crest, giving forcing a broad spectral content (Lavelle et al., 2010; McGillicuddy et al., 2010). A year's average of along-ridge flow over idealized along-ridge-invariant EPR

topography from the two-dimensional model shows (Figure 2a) narrow jets on both sides of the ridge extending almost to the seafloor and to several hundred meters above the ridge crest, as did the current observations at 10 km to the west of the axis (Thurnherr et al., 2011). Yearlong average mean speeds reach 5 cm s⁻¹ and the jets extend as much as 15 km off axis. A month-long average of the along-ridge flow from the model and the along-isobath flow from the off-axis profiling current meter show their comparable magnitude (Figure 2b). The three-dimensional model meridional flow at the profiling current meter site 10 km to the west of the ridge, when weekly averaged, exhibited profiles with speeds and time sequencing comparable

to the weekly averaged along-isobath observations, including a maximum current core speed during one week of 8–10 cm s⁻¹ (Lavelle et al., 2010; Thurnherr et al., 2011). In comparison, the measured amplitudes of the principal lunar tidal current (M₂) at stations 33 km west of and just above the ridge were 2.6 cm s⁻¹ and 4.7 cm s⁻¹, respectively. Moreover, the models show that the jets' size (e.g., width) and speed (e.g., maximum) vary with the strength and orientation of background regional flow, that the jet on one flank at any one time is typically much stronger than the other (e.g., Figure 1), and that location of the stronger jet alternates back and forth across the ridge. Model hydrography dances about the ridge in the time-varying flow, showing alternating uplifted and depressed isopycnals on opposite sides below the crest and doming above it, just as the observation snapshot shows. The models also predict a weak secondary circulation cell with flow downward in the few hundred meters above the ridge crest (Figure 3), but estimated magnitudes of this downward flow at the EPR ($w = 0.1\text{--}0.5\text{ mm s}^{-1}$; recent work of author Lavelle) would make it difficult to measure.

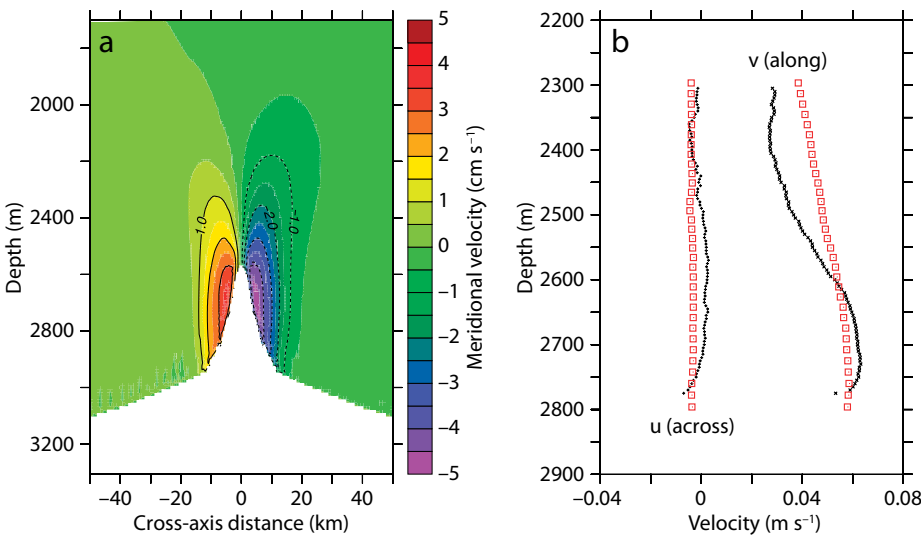


Figure 2. (a) A yearlong average of model meridional flow (positive northward) over an idealized East Pacific Rise (EPR) ridge subject to oscillatory forcing, based on yearlong currents recorded at the EPR (recent work of author Lavelle). The near antisymmetry of these jets is a result of the long averaging interval. Over shorter periods, jet flow is either dominantly poleward or equatorward, depending on the orientation of long-period regional background currents. Over those shorter time periods, the EPR jet can be wider and travel at larger maximum speeds than these averages. (b) Observed (black) and modeled (red) across- and along-topography time-averaged (November 13–December 10, 2006) currents on the western ridge flank ~ 10 km off axis. Whereas the *u* (positive eastward) and *v* (positive northward) coordinates of the two-dimensional model are aligned with the across- and along-ridge directions by construction, steering by isobaths more local to the mooring has been accounted for by rotating the observed currents into a coordinate system aligned with the time-averaged flow direction (320° true) (Thurnherr et al., 2011).

THE UNDERLYING CAUSAL MECHANISMS

The upward-bowing temperature and salinity isolines above the EPR ridge crest lead to density contours that do the same, schematically shown in Figure 3. Water is just slightly colder, more saline, and denser at points directly above the crest compared to water at the same depth off axis. Density surfaces that are not level, like these, support

horizontal pressure gradients, which in turn cause flow. Over long periods, pressure-gradient forces in the ocean are primarily balanced by Coriolis forces, which arise as a consequence of using a rotating coordinate system (Earth-fixed) to describe motion. The simple balance of pressure gradient and Coriolis forces is named geostrophy, a term that combines the Greek “geo” and “strophe” (turning), alluding to Earth’s rotation. Under geostrophy, east-west pressure gradients are balanced by Coriolis forces proportional to north-south currents, such as the EPR jets. The two-dimensional model suggests that the jets are, for the most part, in balance with the domed hydrography via geostrophy. Within about 3 km of the crest, however, the balance of forces also involves nonlinear advection (recent work of author Lavelle), by which oscillatory motion, regardless of stratification, is partly converted into unidirectional motion (i.e., rectification; e.g., Loder, 1980). The spatial scales and magnitudes

of flows generated by hot, buoyant hydrothermal venting are much smaller than those of the jets.

Although geostrophy provides much of the explanation for jets’ existence, it does not explain the doming of the hydrographic distributions underlying the geostrophy. As it turns out, doming of isopycnals (e.g., Figure 3) above the crest is also caused by the oscillatory flow. When the distribution of temperature, for example, is examined using the two-dimensional model’s heat transport equation, variations of velocity and temperature about their time-mean values (i.e., their variance) play an important role. Gradients of the time-averaged products of those velocity and temperature fluctuations serve as a sink for the steady (time-averaged) temperature (heat) distribution (recent work of author Lavelle). Over a zone several hundred meters high above the ridge crest, the heat sink reduces the temperature ever so slightly and the result is upward bowing of isotherms

above the crest. Analogous terms in the salinity transport equation act as sources, so the salinity is slightly bowed upward over the crest as well. As a consequence, isopycnals also dome above the ridge crest. It is oscillatory motion over the ridge that bows the hydrography upward, and then geostrophy that links the hydrography and the jets. Setting aside the less-contributory nonlinear advection mechanism for jet creation at this site, the existence of jets can be traced to the interplay of oscillatory motion, abrupt topography, and stratification, so these ridge jets are examples of “stratified topographic flow rectification.”

Flow steered by topography has a rich history of investigation, a history much too large to summarize here (for entry to the literature, see Brink, 2010, and the references therein). That history includes an approach to the modeling of such flows couched in a formalism different from the primitive equation approach underlying the discussion above. Those studies begin

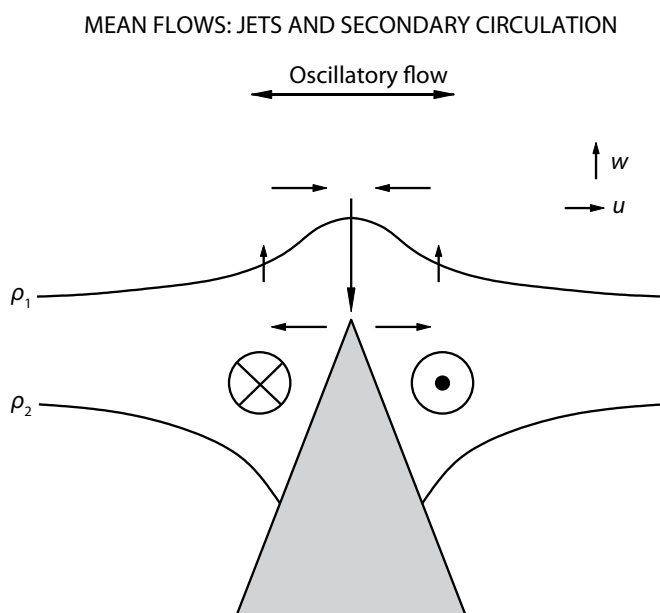


Figure 3. An idealization of circulation and hydrography over a ridge subject to oscillatory flow. The circles with the center dot and the center \times represent flow out of and into the page, respectively. Jets trapped to the ridge flow are directionally sheared across the ridge in an anticyclonic sense (clockwise [counterclockwise] in the Northern [Southern] Hemisphere). Associated with the jets is a very weak mean secondary circulation flowing downward (w) above and outward (u) from the crest, with compensating return flows. The mean diapycnal flux suggested by this circulation is primarily balanced by fluxes arising from the nonzero correlations of oscillating components. Density (ρ) contours bulge upward above the crest and plunge downward into the ridge flanks, though typically only on one side at a time. The symmetry/antisymmetry depicted here represents long-term average conditions only.

with a potential vorticity (PV) equation, where, in one form, PV is defined as a ratio of twice the absolute rate of rotation of a theoretical fluid parcel divided by the parcel height or, if the fluid is stratified, density (e.g., Müller, 1995; Haidvogel and Beckmann, 1999). Using a PV balance equation as a starting point (e.g., Bretherton and Haidvogel, 1976) has advantages of interpretation in some problems because PV conservation has an analog in the conservation of angular momentum. Pertinent examples of the PV approach are found in papers by Vallis and Maltrud (1993), who examined the formation of jets over ridges, and Zimmerman (1980), who studied tidally induced residual flows over irregular topography, both under homogeneous flow conditions. Because the equation set from which the PV balance equation is derived is the primitive equation set, the PV and primitive equation approaches provide equivalent but alternative strategies for studying topographically controlled flow.

SIGNIFICANCE IN THE ABYSSAL OCEAN AND IN A BROADER CONTEXT

On ocean-basin scales, the jets are small in size and flux, but their significance looms large along hydrothermally active mid-ocean ridges. Because jet velocities are relatively large for the deep ocean and jets are trapped along the ridge flanks over long distances, jets may be the principal carriers of biological materials (e.g., Adams et al., 2012, in this issue) between hydrothermal habitats along a ridge segment. If a planktonic larval duration of roughly 30 days for vent species is assumed, currents as strong as those in the jets can transport

larvae over distances approaching the length of ridge segments within the larval stage. McGillicuddy et al. (2010) point out an intriguing and counterintuitive role of jets in larval transport. Only larvae that remain near the seafloor

rather than be returned to the equatorward jet (Lavelle et al., 2010). Because flank jets are so limited in lateral and vertical extent, a deep-ocean advective link of water masses such as this may go unrepresented in global ocean

“ IN VIEW OF THE FACT THAT MID-OCEAN RIDGE SPREADING CENTERS LACE THE WORLD’S OCEAN OVER A DISTANCE OF 67,000 KM, RIDGE JETS MAY YET PROVE TO BE A FACTOR IN ABYSSAL OCEAN HYDROLOGIC, CHEMICAL, AND BIOLOGICAL RESERVOIR CONNECTIVITY AND, THUS, DEEP-OCEAN STIRRING. ”

are carried long distances in jets; those that rise a few hundred meters off the ridge move above the influence of jets and tend to remain near their natal populations. Mechanisms for biological connectivity of neighboring ridge segments across transform faults like the Clipperton and Siqueiros (Figure 1), for example, still must be studied, but the jets will have already influenced the larval reservoir available for those inter-ridge exchanges.


Ridge-associated jets may also play a role in stirring the global ocean at ridge depths. Imagine fluid from one end of a ridge segment being transported in the jet to the opposite end (Figure 1) where it mixes with the local surrounding ocean. Model calculations showed a passive tracer that reached the northern end of the EPR 9–10°N segment in the poleward jet, for example, would continue north into the abyss

models at present-day model resolution (Merryfield and Scott, 2007). In view of the fact that mid-ocean ridge spreading centers lace the world’s ocean over a distance of 67,000 km, ridge jets may yet prove to be a factor in abyssal ocean hydrologic, chemical, and biological reservoir connectivity and, thus, deep-ocean stirring.

Analogs to ridge-rectified flow occur in other ocean settings: at seamounts (e.g., Brink, 1995; Lavelle and Mohn, 2010) and submarine banks (e.g., Loder, 1980; Loder and Wright, 1985; Chen and Beardsley, 1995). These sites are where oscillatory flow and stratification meet steep topography. Observations at seamounts, exemplified by those reported by Brink (1995), show a “cold dome” over the summit and an anticyclonic mean flow trapped to the seamount at the cap level. Brink’s (1995) observations were too sparse, however,

to decipher completely the underlying mechanisms of rectification. In another example, Loder (1980) and Chen and Beardsley (1995), among others, examined anticyclonic flow around Georges Bank, a large, shallow (50 m depth) plateau off the Atlantic coast of North America. Chen and Beardsley (1995) found that tidal forcing alone could reproduce the observed steady flow, one half of which was caused by nonlinear advection and the other half by geostrophy, in which density contours and thus their gradients were set up by “tidal mixing.” As in the case of ridges, these situations and their physics involve oscillatory flow, abrupt topography, nonlevel density structure, geostrophic balances, nonlinear flow interactions, and anticyclonic residual flow.

ACKNOWLEDGMENTS

We thank Richard Thomson for comments on the manuscript that led to its improvement. JWJ is supported by the National Oceanic and Atmospheric Administration (NOAA) Pacific Marine Environmental Laboratory and by NOAA Vents Program. The work of other authors has been supported by National Science Foundation through grants OCE-0424953 and OCE-0425361, LADDER (LARval Dispersion along the Deep East Pacific Rise). This is contribution 3741 from NOAA Pacific Marine Environmental Laboratory. 

REFERENCES

Adams, D.K., S.M. Arellano, and B. Govenar. 2012. Larval dispersal: Vent life in the water column. *Oceanography* 25(1):256–268, <http://dx.doi.org/10.5670/oceanog.2012.24>.

Allen, S.E., and R.E. Thomson. 1993. Bottom-trapped subinertial motions over midocean ridges in a stratified rotating fluid. *Journal*

of Physical Oceanography 23(3):566–581, [http://dx.doi.org/10.1175/1520-0485\(1993\)023<0566:BTSMOM>2.0.CO;2](http://dx.doi.org/10.1175/1520-0485(1993)023<0566:BTSMOM>2.0.CO;2).

Bretherton, F.P., and D.B. Haidvogel. 1976. 2-dimensional turbulence above topography. *Journal of Fluid Mechanics* 78(5):129–154, <http://dx.doi.org/10.1017/s002211207600236x>.

Brink, K.H. 1995. Tidal and lower frequencies above Fieberling Guyot. *Journal of Geophysical Research* 100:10,817–10,832, <http://dx.doi.org/10.1029/95JC00998>.

Brink, K.H. 2010. Topographic rectification in a forced, dissipative, barotropic ocean. *Journal of Marine Research* 68(3–4):337–368, <http://dx.doi.org/10.1357/002224010794657209>.

Cannon, G.A., and D.J. Pashinski. 1997. Variations in mean currents affecting hydrothermal plumes on the Juan de Fuca Ridge. *Journal of Geophysical Research* 102:24,965–24,976, <http://dx.doi.org/10.1029/97JC01910>.

Cannon, G.A., D.J. Pashinski, and M.R. Lemon. 1991. Middepth flow near hydrothermal venting sites on the southern Juan de Fuca Ridge. *Journal of Geophysical Research* 96:12,815–12,831, <http://dx.doi.org/10.1029/91JC01023>.

Chen, C.C., and R.C. Beardsley. 1995. A numerical study of stratified tidal rectification over finite-amplitude banks: Part 1. Symmetrical banks. *Journal of Physical Oceanography* 25(9):2,090–2,110, [http://dx.doi.org/10.1175/1520-0485\(1995\)025<2090:ANSOST>2.0.CO;2](http://dx.doi.org/10.1175/1520-0485(1995)025<2090:ANSOST>2.0.CO;2).

Haidvogel, D.B., and A. Beckmann. 1999. *Numerical Ocean Circulation Modeling*. Imperial College Press, London, 320 pp.

Jackson, P.R., J.R. Ledwell, and A.M. Thurnherr. 2010. Dispersion of a tracer on the East Pacific Rise (9°N to 10°N), including the influence of hydrothermal plumes. *Deep-Sea Research Part I* 57:37–52, <http://dx.doi.org/10.1016/j.dsr.2009.10.011>.

Lavelle, J.W., and G.A. Cannon. 2001. On subinertial oscillations trapped by the Juan de Fuca Ridge, Northeast Pacific. *Journal of Geophysical Research* 106(C12):31,099–31,116, <http://dx.doi.org/10.1029/2001JC000865>.

Lavelle, J.W., and C. Mohn. 2010. Motion, commotion, and biophysical connections at deep ocean seamounts. *Oceanography* 23(1):90–103, <http://dx.doi.org/10.5670/oceanog.2010.64>.

Lavelle, J.W., A.M. Thurnherr, J.R. Ledwell, D.J. McGillicuddy, and L.S. Mullineaux. 2010. Deep ocean circulation and transport where the East Pacific Rise at 9–10°N meets the Lamont seamount chain. *Journal of Geophysical Research* 115, C12073, <http://dx.doi.org/10.1029/2010JC006426>.

Loder, J.W. 1980. Topographic rectification of tidal currents on the sides of Georges Bank. *Journal of Physical Oceanography* 10:1,399–1,416, [http://dx.doi.org/10.1175/1520-0485\(1980\)010<1399:TROTCO>2.0.CO;2](http://dx.doi.org/10.1175/1520-0485(1980)010<1399:TROTCO>2.0.CO;2).

Loder, J.W., and D.G. Wright. 1985. Tidal rectification and frontal circulation on the sides of Georges Bank. *Journal of Marine Research* 43:581–604, <http://dx.doi.org/10.1357/002224085788440367>.

Marsh, A.G., L.S. Mullineaux, C.M. Young, and D.T. Manahan. 2001. Larval dispersal potential of the tubeworm *Riftia pachyptila* at deep-sea hydrothermal vents. *Nature* 411:77–80, <http://dx.doi.org/10.1038/35075063>.

McGillicuddy, D.J. Jr., J.W. Lavelle, A.M. Thurnherr, V.K. Kosnyrev, and L.S. Mullineaux. 2010. Larval dispersion along an axially symmetric mid-ocean ridge. *Deep-Sea Research Part I* 57(7):880–892, <http://dx.doi.org/10.1016/j.dsr.2010.04.003>.

Merryfield, W.J., and R.B. Scott. 2007. Bathymetric influence on mean currents in two-high resolution near-global models. *Ocean Modelling* 16:76–94, <http://dx.doi.org/10.1016/j.ocemod.2006.07.005>.

Müller, P. 1995. Ertel's potential vorticity theorem in physical oceanography. *Reviews of Geophysics* 33(1):67–97, <http://dx.doi.org/10.1029/94RG03215>.

Mullineaux, L.S., D.K. Adams, S.W. Mills, and S.E. Beaulieu. 2010. Larvae from afar colonize deep-sea hydrothermal vents after catastrophic eruption. *Proceedings of the National Academy of Sciences of the United States of America* 107:7,829–7,834, <http://dx.doi.org/10.1073/pnas.091318710>.

Thomson, R.E., S.E. Roth, and J. Dymond. 1990. Near-inertial motions over a mid-ocean ridge: Effects of topography and hydrothermal plumes. *Journal of Geophysical Research* 95(C5):7,261–7,278, <http://dx.doi.org/10.1029/jc095ic05p07261>.

Thurnherr, A.M., J.R. Ledwell, J.W. Lavelle, and L.S. Mullineaux. 2011. Hydrography and circulation near the crest of the East Pacific Rise between 9° and 10°N. *Deep-Sea Research Part I* 58(4):365–376, <http://dx.doi.org/10.1016/j.dsr.2011.01.009>.

Vallis, G.K., and M.E. Maltrud. 1993. Generation of mean flows and jets on a beta-plane and over topography. *Journal of Physical Oceanography* 23(7):1,346–1,362, [http://dx.doi.org/10.1175/1520-0485\(1993\)023<1346:GOMFAJ>2.0.CO;2](http://dx.doi.org/10.1175/1520-0485(1993)023<1346:GOMFAJ>2.0.CO;2).

Watson, A.J., and J.R. Ledwell. 2000. Oceanographic tracer release experiments using sulphur hexafluoride. *Journal of Geophysical Research* 105:14,325–14,337, <http://dx.doi.org/10.1029/1999JC900272>.

Zimmerman, J.T.F. 1980. Vorticity transfer by tidal currents over an irregular topography. *Journal of Marine Research* 38(4):601–630.